Cell

Brd4 and JMJD6-Associated Anti-Pause Enhancers in Regulation of Transcriptional Pause Release

Wen Liu,[1,2,5,*] Qi Ma,[1,3,5] Kaki Wong,[1] Wenbo Li,[1] Kenny Ohgi,[1] Jie Zhang,[1] Aneel K. Aggarwal,[4] and Michael G. Rosenfeld[1,*]

[1]Howard Hughes Medical Institute, Department of Medicine, School of Medicine, University of California, San Diego, 9500 Gilman Drive, La Jolla, CA 92093, USA

[2]School of Pharmaceutical Science, Xiamen University, Xiang'an South Road, Xiamen, Fujian 361102, China

[3]Graduate Program in Bioinformatics and System Biology, University of California San Diego, 9500 Gilman Drive, La Jolla, CA 92093, USA

[4]Department of Structural and Chemical Biology, Mount Sinai School of Medicine, Box 1677, 1425 Madison Avenue, New York, NY 10029, USA

[5]These authors contributed equally to this work

*Correspondence: w2liu@xmu.edu.cn (W.L.), mrosenfeld@ucsd.edu (M.G.R.)

http://dx.doi.org/10.1016/j.cell.2013.10.056

SUMMARY

Distal enhancers characterized by the H3K4me[1] mark play critical roles in developmental and transcriptional programs. However, potential roles of specific distal regulatory elements in regulating RNA polymerase II (Pol II) promoter-proximal pause release remain poorly investigated. Here, we report that a unique cohort of jumonji C-domain-containing protein 6 (JMJD6) and bromodomain-containing protein 4 (Brd4) cobound distal enhancers, termed *a*nti-*p*ause *e*nhancers (A-PEs), regulate promoter-proximal pause release of a large subset of transcription units via long-range interactions. Brd4-dependent JMJD6 recruitment on A-PEs mediates erasure of H4R3me[2(s)], which is directly read by 7SK snRNA, and decapping/demethylation of 7SK snRNA, ensuring the dismissal of the 7SK snRNA/HEXIM inhibitory complex. The interactions of both JMJD6 and Brd4 with the P-TEFb complex permit its activation and pause release of regulated coding genes. The functions of JMJD6/ Brd4-associated dual histone and RNA demethylase activity on anti-pause enhancers have intriguing implications for these proteins in development, homeostasis, and disease.

INTRODUCTION

The critical roles of enhancers have been recognized for more than 25 years, and recently the H3K4me[1] mark was identified to characterize many gene enhancers (Heintzman et al., 2009). These enhancers have been recently found to be usually associated with noncoding RNA transcripts called enhancer RNA (Hah et al., 2013; Lam et al., 2013; Li et al., 2013; Natoli and Andrau, 2012; Ren, 2010). The molecular mechanisms underlying transcription regulation by enhancers as well as other distal regulatory elements with enhancer-like properties remain incompletely understood.

JMJD6, also known as PTDSR or PSR, a JmjC-domain-containing protein, has been suggested to possess novel, unexpected nuclear functions (Cui et al., 2004; Tibrewal et al., 2007). Ablation of *JMJD6* in mice caused abnormal development and led to neonatal lethality (Böse et al., 2004; Kunisaki et al., 2004; Li et al., 2003). It was originally identified as a phosphatidylserine receptor on the surface of phagocytes (Fadok et al., 2000). It has been recently reported to be an arginine demethylase and lysyl-5-hydroxylase (Chang et al., 2007; Webby et al., 2009), although the potential functional importance of these activities remains unclear. Meanwhile, a structural study suggested that methyl groups on single-stranded RNAs (ssRNAs) might be substrates of JMJD6 (Hong et al., 2010).

Brd4, along with Brd2, Brd3, and testes/oocyte-specific BrdT, comprises the BET domain family of proteins in mammals, which is characterized by the presence of tandem, amino-terminal bromodomains and an extraterminal (ET) domain. Knockout of *Brd4* and *Brd2* in mice leads to early embryonic lethality (Gyuris et al., 2009; Houzelstein et al., 2002). Small-molecule inhibition of Brd4 has been proposed as a promising therapeutic strategy for certain cancers (Delmore et al., 2011; Filippakopoulos et al., 2010; Nicodeme et al., 2010; Zuber et al., 2011). Brd4 has been found in several complexes, including the mediator and P-TEFb complexes (Jang et al., 2005; Wu et al., 2003; Yang et al., 2005). The P-TEFb complex is a heterodimer consisting of the cyclin-dependent kinase Cdk9 and a cyclin component (Cyclin T1, T2, or K). Brd4 is capable of releasing the P-TEFb complex from the inhibitory factors, HEXIM1/2 and 7SK snRNA, through its direct interaction with Cyclin T1, resulting in the transition of the P-TEFb complex from its inactive to an active form and subsequent phosphorylation of RNA Pol II, leading to efficient transcriptional elongation (Jang et al., 2005; Yang et al., 2005). This positive regulation of the P-TEFb complex is

believed to be vital for Brd4 function (Dey et al., 2009; Hargreaves et al., 2009; Mochizuki et al., 2008; Yang et al., 2008). Enhancer-bound Brd4 regulation of transcription has been recently shown in cancer cells as well as heart failure, although the underlying molecular mechanisms are incompletely understood (Anand et al., 2013; Lovén et al., 2013).

Emerging evidence suggests that promoter-proximal pausing of Pol II is a critical regulatory event subsequent to Pol II initiation on a large set of genes (Adelman and Lis, 2012). Pol II promoter-proximal pause release is achieved mainly through the action of the P-TEFb complex, which phosphorylates at least three targets including the NelfE subunit of NELF, the Spt5 subunit of DSIF, and serine 2 of RNA Pol II carboxyl-terminal domain (CTD) (Kim and Sharp, 2001; Marshall et al., 1996; Wada et al., 1998; Yamada et al., 2006). Half of the total P-TEFb in the cells is reversibly bound to the inhibitory subunit composed of 7SK snRNA and HEXIM1/2 and thus is in an inactive form (Nguyen et al., 2001; Yang et al., 2001), whereas the remaining half associates with Brd4 (Jang et al., 2005; Yang et al., 2005). Although HIV-1 Tat and Brd4 are capable of directly extracting P-TEFb out from its 7SK snRNP inhibitory complex (Krueger et al., 2010), the physiological molecular mechanisms governing the release of P-TEFb complex and transition to the active form remain incompletely understood.

In the present study, we provide evidence that JMJD6 and Brd4 physically and functionally interact in the context of the active P-TEFb complex to regulate Pol II promoter-proximal pause release of a large cohort of genes. The pause release function of the JMJD6 and Brd4 complex on these genes is established primarily based on binding to distal enhancers, which we term as *a*nti-*p*ause *e*nhancers (A-PEs). Mechanistically, 7SK snRNA is found to function as a "reader" for H4R3me$^{2(s)}$, a repressive histone mark, and JMJD6 displays dual demethylase activities toward both H4R3me$^{2(s)}$ and the methyl-cap of 7SK snRNA, resulting in the disassembly of the 7SK snRNA/HEXIM1 inhibitory complex imposed on the P-TEFb complex. Simultaneously, both JMJD6 and Brd4 are capable of retaining the P-TEFb complex through physical interaction with CDK9 and Cyclin T1, respectively, leading to its activation, and eventuating in transcriptional pause release and gene activation.

RESULTS

Physical and Functional Interaction between JMJD6 and Brd4

Initially, identifying JMJD6 interacting partners in HEK293 cell lines revealed the presence of Brd4, with six peptides predicted with high confidence (Figure 1A and Table S1 available online), consistent with previous reports (Rahman et al., 2011; Webby et al., 2009). Accordingly, JMJD6 was found in the list of Brd4-associated proteins, with four peptides predicted with high confidence, strengthening the possibility that these two proteins might function together to regulate cellular process (Figure S1A). In addition, known functional partners of Brd4 were also successfully identified in our pull-down, including the P-TEFb complex composed of Cdk9 and Cyclin T1 (Jang et al., 2005; Rahman et al., 2011). The interaction between JMJD6 and Brd4 or P-TEFb complex, including Cdk9 and Cyclin T1/2, was further confirmed, suggesting that it associates with the active form of P-TEFb complex (Figure 1B). To test whether JMJD6 also associates with the inactive form of the P-TEFb complex, proteins associated with 7SK snRNA were identified. Known 7SK snRNA-associated proteins, including HEXIM1, BCDIN3, LARP7, and the P-TEFb complex (Cdk9 and Cyclin T1), were successfully identified, whereas neither JMJD6 nor Brd4 was detected (Table S2), as further confirmed through immunoblotting (Figure 1C). These data suggest that JMJD6 and Brd4 specifically interact with the active form of the P-TEFb complex.

Direct interaction between JMJD6 and Brd4 was demonstrated in vitro (Figures 1D and S1B) and in HEK293T cells cotransfected with JMJD6 and Brd4 (Figure 1E). The JMJD6 interacting domain in Brd4 was mapped to a fragment harboring the extraterminal domain (ET) (aa 471–730) in vitro (Figures S1C–S1E) and in HEK293T cells (Figure S1F). Similarly, the amino-terminal and JmjC domains of JMJD6 together mediated its interaction with Brd4 both in vitro (Figures S1G–S1L) and in HEK293T cells (Figure S1M).

To begin to examine the transcriptional regulation by JMJD6 and Brd4 in the context of active P-TEFb complex, HEK293T cells were transfected with control small interfering RNA (siRNA) or two independent siRNAs specifically targeting *JMJD6* or *Brd4* followed by Gro-seq analyses (Figures 1F, S2A, and S2B). Each of the two siRNAs targeting *JMJD6* or *Brd4* caused transcriptional changes in a substantial number of genes (Figures 1G, 1H, S2C, and S2D). We subsequently focused on the conserved program (Figures 1G and 1H). In accord with their association with the active P-TEFb complex, 82% of JMJD6- or 71% Brd4-regulated genes exhibited impaired transcription when knocking down of *JMJD6* or *Brd4*, respectively (Figures 1G and 1H). Significantly, over 56% or 47% of the genes regulated by JMJD6 or Brd4, respectively, were jointly regulated by these two proteins (n = 1,201) (Figure 1I and Table S3), 96.2% of which were regulated in the same direction by both proteins (n = 1,155) (Figure 1J). Out of these 1,155 genes, 88% of them required both JMJD6 and Brd4 for transcriptional activation (n = 1,022) (Figure 1J), as further validated by quantitative RT-PCR (qRT-PCR) (Figure S2E). These genes that were positively regulated in common by both JMJD6 and Brd4 (n = 1,022) were referred to as JB genes. Gene ontology analysis revealed that functional terms, including cellular metabolic process, embryonic development, RNA splicing and processing, cell death and apoptosis, cellular localization, and cell-cycle regulation, were enriched (Table S4). Together, our experiments argue in favor of a physical and functional interaction between JMJD6 and Brd4.

Regulation of Pol II Promoter-Proximal Pause Release by JMJD6 and Brd4

Brd4 has been shown to be critical for transcriptional elongation presumably through its recruitment of P-TEFb complex. Based on the fact that JMJD6 and Brd4 coregulated a significant subset of genes, we hypothesized that JMJD6 might also play a role in the process of P-TEFb activation and promoter-proximal Pol II pause release. To test this hypothesis, Pol II chromatin immunoprecipitation sequencing (ChIP-seq) analysis was performed in control siRNA or siRNA specifically targeting *JMJD6*- or

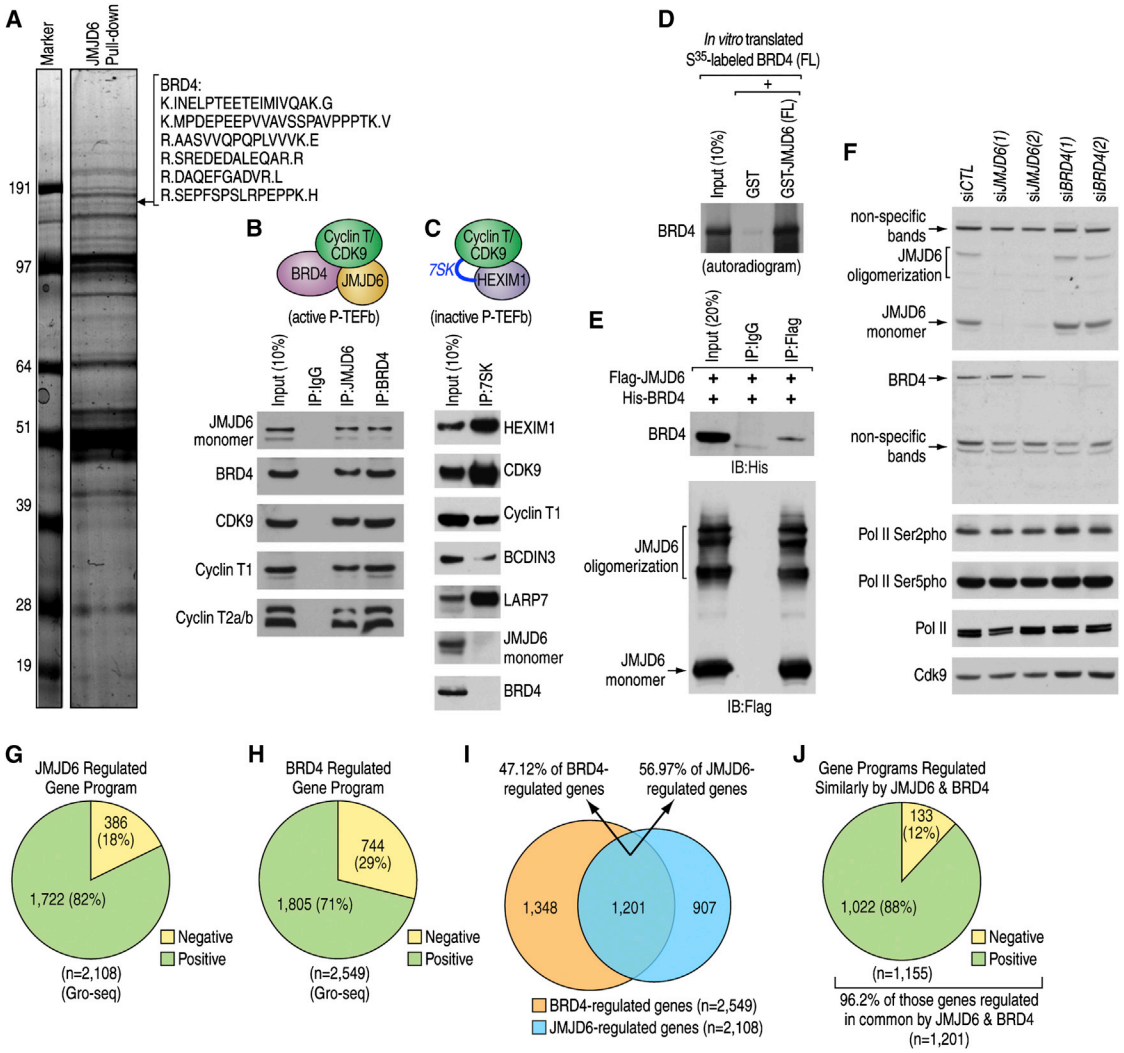

Figure 1. Physical Interaction between JMJD6 and Brd4 in the Context of Active P-TEFb Complex

(A) JMJD6-associated proteins were purified using Flag-affinity agarose, separated by SDS-PAGE gel, stained with Coomassie blue, and then subjected to mass spectrometry analysis. Identified peptides for Brd4 were shown on the right.

(B) Nuclear extracts purified from HEK293T cells were subjected to immunoprecipitation (IP) and followed by immunoblotting (IB).

(C) In vitro 7SK RNA pull-down assay was performed, and the resultant pellet was analyzed by IB.

(D and E) JMJD6 and Brd4 interaction examined through in vitro GST pull-down assay (D) or IP in HEK293T cells (E). Note that JMJD6 undergoes multimerization, which is preserved even under denatured conditions.

(F) HEK293T cells transfected with control siRNA or two independent siRNAs specifically targeting *JMJD6* or *Brd4* were subjected to IB analysis.

(G and H) Pie chart showing genes regulated by JMJD6 (G) or Brd4 (H) assessed by Gro-seq analysis in cells as described in (F) (FDR < 0.001).

(I) Overlap between JMJD6- and Brd4-regulated genes from (G) and (H), respectively.

(J) Genes regulated in common and in the same direction by JMJD6 and Brd4.

See also Figures S1 and S2 and Tables S1, S2, S3, and S4.

Brd4-transfected HEK293T cells. For the vast majority of genes, Pol II occupancy was at a much higher density at the promoter-proximal region compared to gene body (Figure S2F). We then calculated the relative ratio of Pol II density in the promoter-proximal region and the gene body, which has been termed as traveling ratio (TR) (Reppas et al., 2006) or pausing index (Zeitlinger et al., 2007) (Figure 2A). It was found that nearly 90% of Pol-II-bound genes have a TR larger than 2, suggesting that these genes experience promoter-proximal pausing regulation (Figure S2G), a result similar to what was found in embryonic stem (ES) cells (Rahl et al., 2010). When all Pol-II-bound genes were assessed, JMJD6 exhibited only a modest, although significant, effects on TR values, whereas the number of genes and the magnitude of TR changes affected by *Brd4* knockdown was much larger (Figures 2B and 2C). However, when considering only JB genes, we found that knockdown of either protein led to a significant increase of TR values and the changes were in a similar extent, suggesting that these factors coregulate Pol II

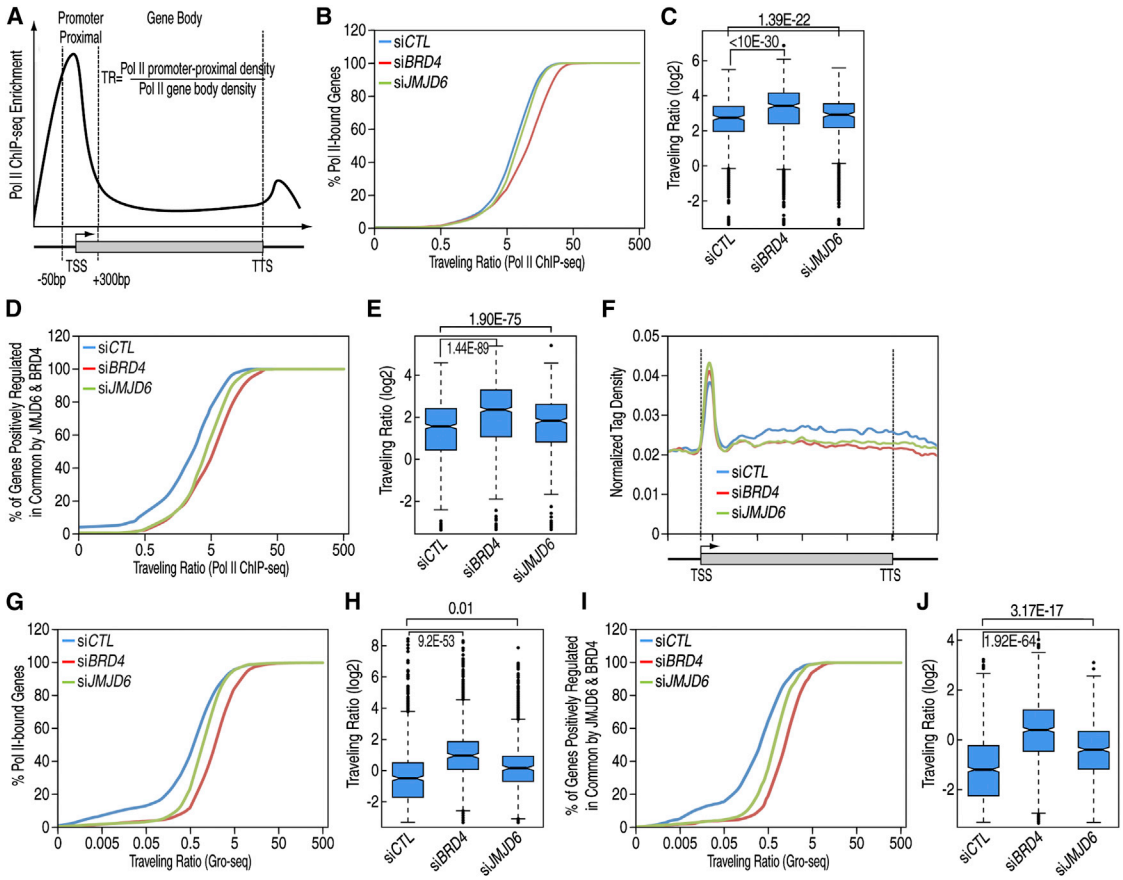

Figure 2. JMJD6 and Brd4 Promote Promoter-Proximal Pol II Pause Release

(A) Schematic representation of the way applied to calculate Pol II traveling ratio (TR).

(B and D) Pol II TR distribution in HEK293T cells for all Pol-II-bound genes (B) or genes that are positively regulated in common by JMJD6 and Brd4 (n = 1,022) (JB genes) (D).

(C and E) Box plots showing the change of Pol II TR caused by knockdown of *JMJD6* or *Brd4* in (B)–(D). (E) Median (C): 6.54 (siCTL), 10.36 (siBrd4), 7.48 (siJMJD6); median (E): 2.61 (siCTL), 5.46 (siBrd4), 4.14 (siJMJD6).

(F) Gro-seq read distribution along the transcription units from 2 kb upstream of the transcription start site (TSS) to 2.5 kb downstream of the transcription termination site (TTS) in HEK293T cells transfected with control, *JMJD6*, or *Brd4* siRNA. Region included was normalized and scaled to 1.

(G and I) TR distribution based on Gro-seq analysis in HEK293T cells for all Pol-II-bound genes (G) or JB genes (I).

(H and J) Box plots showing change of TR caused by knockdown of *JMJD6* or *Brd4* as shown in (G)–(I). (J) Median (H): 0.61 (siCTL), 1.82 (siBrd4), 1.00 (siJMJD6); median (J): 0.33 (siCTL), 1.22 (siBrd4), 0.66 (siJMJD6).

See also Figure S2.

promoter-proximal pause release on these genes (Figures 2D and 2E). Furthermore, the significance of the TR change caused by *JMJD6* or *Brd4* knockdown was comparable to that by DRB or flavopiridol treatment, two P-TEFb inhibitors (Figures S2H and S2I). Specifically, ~85% of those 1,022 genes showed an increase of TR value after knocking down either *JMJD6* or *Brd4* (Figure S2J). The fold change of TR value on a specific gene correlated poorly with its length (Figures S2K and S2L). To further strengthen the idea that both JMJD6 and Brd4 are essential and function in a protein complex to regulate pause release of JB genes, double knockdown of *JMJD6* and *Brd4* displayed no additive effects on TR change compared to knockdown of *JMJD6* or *Brd4* individually (Figure S2M).

In further support of their role in promoting Pol II promoter-proximal pause release, knockdown of *JMJD6* or *Brd4* caused a slight increase of read density at promoter-proximal region but a dramatic decrease along the gene body based on Gro-seq analysis, resembling a typical pause release defect (Figure 2F). By the criterion defining Pol II TR as the relative ratio of Gro-seq reads density in the promoter-proximal region and the gene body, both *JMJD6* and *Brd4* knockdown caused a significantly increased TR compared to control samples when all Pol-II-bound genes were examined, with the magnitude of TR changes caused by *Brd4* knockdown being more dramatic (Figures 2G and 2H). Importantly, ~85% of those 1,022 genes showed an increase of TR value after knocking down either *JMJD6* or *Brd4* (Figures 2I, 2J, and S2N). Similar to analyses based on Pol II ChIP-seq, the fold change of TR value assessed by Gro-seq on a specific gene was poorly correlated with its length (Figures S2O and S2P).

Genomic Localization of JMJD6 and Brd4

ChIP-seq profiling of JMJD6 and Brd4 binding sites across the genome revealed that Brd4 localized on the promoter region of a large set of genes (n = 6,120, ~44% of its total binding sites), with the remaining 56% (n = 7,878) located on intergenic and intragenic regions (Figure 3A). In contrast, JMJD6 was detected on only ~500 promoters, comprising ~6% of all JMJD6 binding sites, with the vast majority of JMJD6 binding sites (n = 7,815) located on intergenic and intragenic regions (Figures 3B and S3A). Identified binding sites for JMJD6 and Brd4 were validated by ChIP-qPCR (Figure S3B). Interestingly, JMJD6 and Brd4 were highly correlated on distal regions (intergenic and intragenic regions) (Figures 3C and S3C). Although Brd4 promoter occupancy was observed on ~53% of those JB genes, only ~3% of them (n = 34) had detectable peaks for JMJD6 (Figure 3D). Indeed, the ChIP-seq tag density for JMJD6 was close to background at the promoter regions of those JB genes (Figures 3E and 3F). These observations raised the intriguing possibility that JMJD6, with Brd4, might regulate Pol II promoter-proximal pause release for the subset of genes they jointly regulated in an unexpected distal regulatory fashion, which would be most likely established via long-range interactions between promoters and JMJD6 and Brd4 co-occupied distal sites (Figure 7K).

Characterization of JMJD6 and Brd4 Co-Occupied Distal Sites

To test whether JMJD6 and Brd4 cobound distal sites might correspond to current definitions of enhancers, we performed ChIP-seq for several histone marks and coactivators, finding that they were enriched with H3K4me$^{1/2}$, H3K27Ac, and P300 but exhibited low/no levels of H3K4me^{3}, features characteristic of active enhancers (Figures 3E and 3F). We hypothesized that Brd4 recognition of acetylated histones was likely to account for the recruitment of the Brd4 and JMJD6 complex to their co-occupied enhancers because the two bromodomains of Brd4 are well established to bind to acetylated histone tails, mainly focusing on diacetylated H3 (K9 and K14) (H3Ac) or tetraacetylated H4 (K5, 8, 12, and 16) (H4Ac). Indeed, ~95% of Brd4 binding regions and ~90% of JMJD6 and Brd4 cobound distal enhancers were enriched with either H3Ac or H4Ac marks (Figures S3D, S3E, and 3E–3G). To support the requirement of Brd4 for JMJD6 binding, it was found that JMJD6 binding decreased significantly following knockdown of *Brd4* on randomly selected JMJD6 and Brd4 cobound distal enhancers (Figure 3H); however, knockdown of *JMJD6* exerted no significant effects on Brd4 binding (Figure 3I).

H4R3me$^{2(s)}$ Demethylase Activity of JMJD6

To explore how the recruitment of the JMJD6 and Brd4 protein complex to their co-occupied distal enhancers functionally links to the regulation of Pol II promoter-proximal pause release, we first examined JMJD6 histone demethylase activity. It was found that, in contrast to the enzymatically dead mutant, wild-type JMJD6 purified from bacterial cells specifically demethylated methylated histone H4R3, including mono- (H4R3me^{1}), symmetric di-(H4R3me$^{2(s)}$), and asymmetric di-(H4R3me$^{2(a)}$) forms, but not other methylated arginine or lysine residues examined. Total levels of histone H3 and H4 remained unchanged (Figures 4A, S3F, and S3G). An interacting ssRNA (Hong et al., 2010), its sense or antisense form, was included in our demethylase assay, finding that it exerted no effects on JMJD6 enzymatic activity (Figure 4A). To examine JMJD6 regulation by posttranslational modifications (PTMs) or functionally associated protein partners, we performed in vitro histone demethylase assays by using Flag-tagged JMJD6 or its enzymatically dead mutant (H187A) purified from HEK293T cells following overexpression. Again, JMJD6 displayed a specific demethylase activity toward H4R3me, but not H4K20me or other arginine or lysine methylations examined. In contrast, the enzymatically dead JMJD6 mutant (H187A) had no effect on any histone modifications examined (Figures 4B and S3H; data not shown). RNaseA was also included in the demethylation reactions to remove any RNA copurified with the enzyme, finding that it had no effect on JMJD6 enzymatic activities (Figure 4B). Furthermore, JMJD6 demethylase activity toward H4R3me was confirmed using histone tail peptides as substrates (Figure S3I).

As H4R3me$^{2(s)}$ and its methyltransferase, PRMT5, have been suggested to associate with transcriptional repression, we focused on the demethylase activity of JMJD6 toward this histone mark in this current study (Wysocka et al., 2006; Xu et al., 2010). To further support JMJD6 demethylase activity toward H4R3me$^{2(s)}$, a significant change of H4R3me$^{2(s)}$ occupancy was observed on JMJD6 and Brd4 cobound distal enhancers upon *JMJD6* knockdown (Figures 4C and 4D), but not on the promoter regions of those JB genes (Figure 4E). Because histone modifications exert effects through recruiting "reader" proteins or noncoding RNAs (Lachner et al., 2003; Ruthenburg et al., 2007; Yang et al., 2011), we speculated that JMJD6 demethylation of the repressive H4R3me$^{2(s)}$ mark, which might be read by 7SK snRNA and HEXIM1/2, would result in the disassembly of the inhibitory complex imposed on P-TEFb complex. Probing MODified Histone Peptide Array with purified HEXIM1 protein revealed no specific binding to modified histone tails (data not shown). Intriguingly, 7SK snRNA was found to associate with several histone peptides on the array, with enrichment of H4R3me^{2}, as well as H4K5Ac, H4K8Ac, H4K12Ac, and H4K16Ac modifications (Figures 4F, S3J, and S3K). In vitro RNA pull-down confirmed that 7SK snRNA specifically associated with nucleosomes enriched for H4R3me^{2} or H4Ac (K5, 8, 12, and 16), but not H3R2me^{2} or H3Ac (K9 and 14) (Figure 4G). Furthermore, H4R3me$^{2(s)}$-containing histone tails were found to specifically associate with the 5′-, but not 3′-terminal half of 7SK (Figures 4H and S3L). Together, these data suggest that JMJD6-mediated demethylation of H4R3me$^{2(s)}$, a repressive histone mark directly read by 7SK snRNA, can potentially result in the dismissal of 7SK snRNA/HEXIM1 inhibitory complex and subsequent P-TEFb complex activation and transcriptional pause release (Figure 7K).

A 7SK snRNA Decapping Function of JMJD6

7SK snRNA is capped posttranscriptionally through the addition of a methyl group directly on the gamma-phosphate of its first 5′ nucleotide by its capping enzyme, BCDIN3/MePCE (Jeronimo et al., 2007). The cap structure enhances the stability of 7SK snRNA by protecting the RNA from exonucleolytic degradation (Jeronimo et al., 2007; Shumyatsky et al., 1990). As a recent

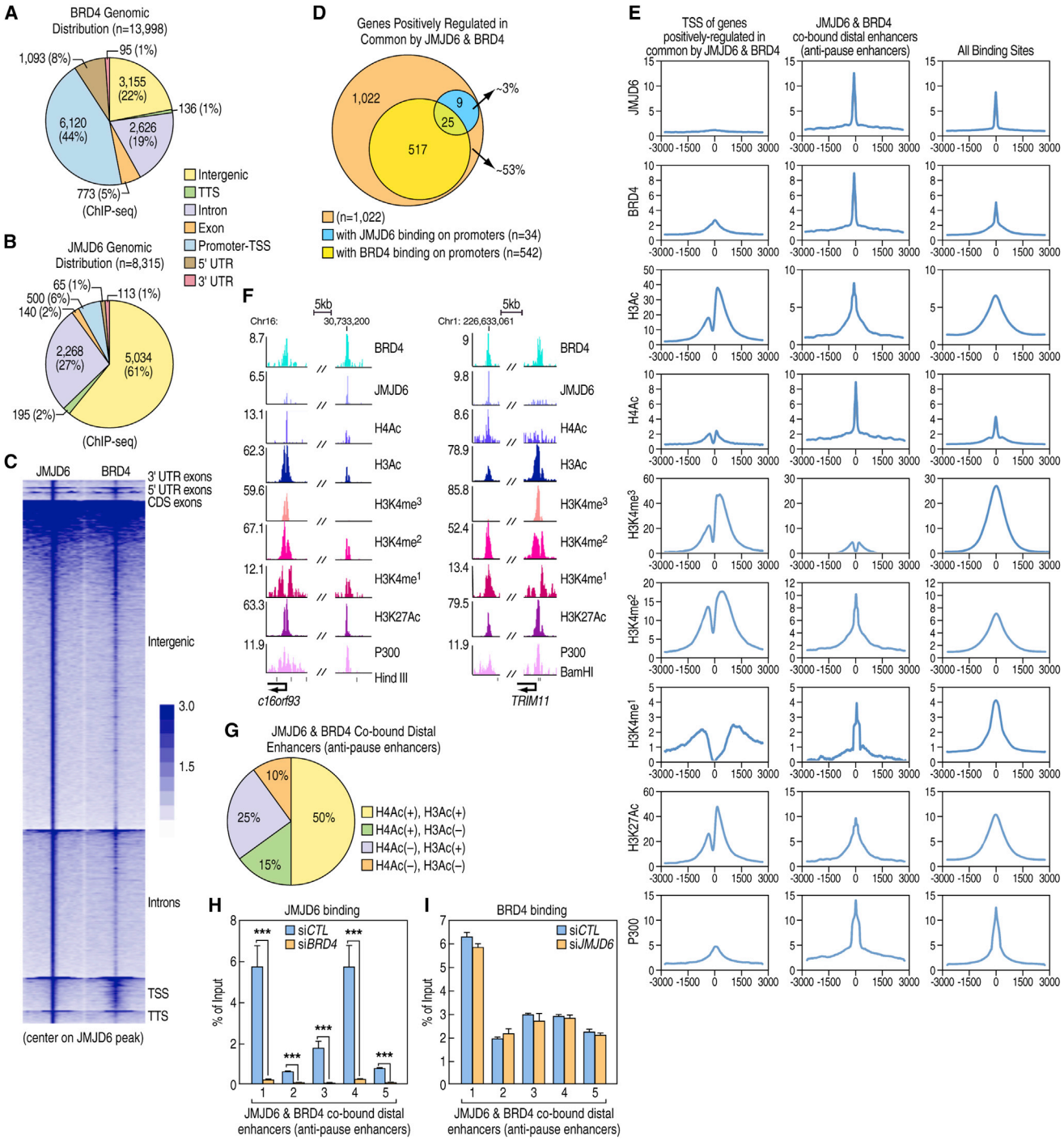

Figure 3. JMJD6 and Brd4 Genomic Binding

(A and B) Genomic distribution of Brd4 (A) or JMJD6 (B) binding sites.

(C) Heatmap representation of JMJD6 and Brd4 tag density centered on JMJD6 ChIP-seq peaks.

(D) Venn diagram showing the number of genes having JMJD6 and/or Brd4 binding on promoter regions among those JB genes.

(E) ChIP-seq tag distribution of JMJD6, Brd4, H3Ac, H4Ac, H3K4me^3, H3K4me^2, H3K4me^1, H3K27Ac, or P300 surrounding TSS of those JB genes (left), the center of JMJD6 and Brd4 cobound distal sites (middle), or all of its own binding sites in the genome (right).

(F) JMJD6, Brd4, H3Ac, H4Ac, H3K4me^3, H3K4me^2, H3K4me^1, H3K27Ac, or P300 binding on selected genomic regions: *C16orf93* or *TRIM11* promoter region and the nearby JMJD6 and Brd4 cobound distal enhancer (center of enhancer: chr16:30,733,200 [left]; chr1:226,633,061 [right]).

(G) Pie chart displaying the percentage of JMJD6 and Brd4 cobound distal sites with or without H4Ac or H3Ac marks.

(legend continued on next page)

structural study suggested that methyl group on ssRNA might serve as substrate of JMJD6 (Hong et al., 2010), we hypothesized that JMJD6 might possess a novel activity toward the methyl group in the cap structure of 7SK snRNA, which could result in 7SK snRNA destabilization and subsequent P-TEFb activation. Indeed, BCDIN3 efficiently methylated 7SK snRNA, and the methylation signals decreased in a dose-dependent manner in the presence of JMJD6 (Figures 4I and S3M). Furthermore, demethylation of 7SK snRNA by JMJD6 was dependent on its JmjC domain (Figure S3N). Surprisingly, neither *JMJD6* nor *Brd4* knockdown resulted in a significant change of total 7SK snRNA levels assessed by northern blotting in cells, suggesting JMJD6 demethylation of 7SK snRNA might occur locally on chromatin (Figure S3O). 7SK snRNA ChIRP was then performed using a single DNA oligonucleotide, which was shown to specifically target and efficiently pull down 7SK snRNA (Yang et al., 2001). Indeed, around 85% of total cellular 7SK snRNA was retrieved, but not GAPDH mRNA (Figure 4J). Knockdown of *BCDIN3* led to a significant decrease of the tags of our identified 7SK binding peaks ($p < 10E-100$), further supporting specificity of the 7SK ChIRP. Consistent with our hypothesis, 7SK snRNA occupancy increased significantly on JMJD6 and Brd4 cobound distal enhancers following *JMJD6* or *Brd4* knockdown, but not on the promoter regions of those JB genes (Figures 4K and S3P). Increased HEXIM1 binding was also observed for a number of JMJD6 and Brd4 cobound distal enhancers tested by conventional ChIP (Figure 4L). We therefore have coined a presumptive designation for the JMJD6 and Brd4 cobound distal enhancers, referring to them as *anti-p*ause *e*nhancers (A-PEs), on which JMJD6 displays demethylation activity toward H4R3me$^{2(s)}$ and methyl group in the 7SK snRNA cap.

Anti-Pause Enhancers Loop to and Regulate Pausing Release of Target Gene Promoters

To test the hypothesis that JMJD6 regulation of Pol II promoter-proximal pause release would be established via long-range interactions between promoters and anti-pause enhancers (A-PEs), chromosome conformation capture (3C) analysis was performed for a number of genes, which were strongly regulated by JMJD6 and Brd4, including *SAMD11*, *ALDOA*, *RHOB*, *CHKB*, *C16orf93*, and *TRIM11*, all of which showed specific interactions with their nearby cognate A-PEs (Figures 5A–5C and S4A–S4C). Intriguingly, the detected interactions were generally not significantly affected by either JMJD6 or Brd4, suggesting that they were established based on other enhancer-bound factors, regardless of gene expression status. The striking presence of nine subunits of the mediator complex in our MS analysis for proteins associated with JMJD6, including MED1 (Table S1), co-occupancy of Brd4 with MED1 on enhancers and promoters in several cancer cell lines, and mediators' roles in functionally connecting enhancers and core promoters of many active genes prompted us to test whether MED1 affects looping formation between gene promoters and A-PEs (Kagey et al., 2010; Lovén et al., 2013). Indeed, knockdown of *MED1* impaired the looping formation for all gene promoters and A-PEs tested (Figures 5A–5C and S4A–S4C).

To further demonstrate that A-PEs are functionally linked to transcriptional control of these coding genes, selected promoter regions were cloned with corresponding A-PEs into pGL3 basic luciferase vectors and transfected into HEK293T cells. For all ten constructs tested, the combination of promoter sequence and anti-pause enhancer (P+A-PE) drove the luciferase gene expression efficiently, which was impaired following knockdown of either *JMJD6* or *Brd4* (Figures 5D–5F and S4D–S4J, far right three columns). To support the notion that A-PEs regulate transcription at the Pol II promoter-proximal pause release step, Pol II ChIP analysis revealed that the relative ratio of Pol II density in the promoter-proximal region and two selected regions on the luciferase gene body increased significantly following knockdown of *JMJD6* or *Brd4*, suggesting a defect in Pol II pause release (Figures 5G and 5H). Interestingly, the luciferase reporter activities detected from vectors containing promoter sequences only (P), presumably lacking of 7SK snRNA/HEXIM inhibitory complex associated with A-PEs, was significantly lower than vectors containing both promoter sequences and A-PEs (P+A-PE), suggesting that JMJD6 and Brd4 might have additional roles, such as retaining the P-TEFb complex, besides their function in dismissing the inhibitory 7SK snRNA/HEXIM complex (Figures 5D–5F and S4D–S4J). Consistent with this, the relative ratio of Pol II density in the promoter-proximal region and selected region in the body of luciferase gene detected from luciferase vector containing promoter sequence only (P) was significantly larger than that from luciferase vectors containing both promoter sequence and A-PE (P+A-PE) (Figures 5G and 5H).

Activation of the P-TEFb Complex by JMJD6 and Brd4

Our data suggested that JMJD6 and Brd4 might retain and activate the P-TEFb complex in addition to dismissing 7SK snRNA/HEXIM. Because Brd4 is known to interact with the Cyclin T1 in the P-TEFb complex and to be capable of extracting the P-TEFb complex from 7SK snRNP (Jang et al., 2005; Krueger et al., 2010; Yang et al., 2005), we investigated whether JMJD6 might play a similar role. JMJD6 was found to specifically interact with CDK9, but not with Cyclin T1 (Figures 6A, 6B, and S5A). Both the amino-terminal and the JmjC domain of JMJD6 were able to interact with CDK9, whereas carboxyl-terminal, containing the unstructured region, failed to do so (Figures S5B and S5C). The carboxyl-terminus (aa 315–372) of CDK9 was apparently required for its binding with JMJD6 as any truncations lacking this region failed to bind (Figure S5D), but sufficiency could not be tested because it alone was not expressed in cells. Therefore, our data and those from previous studies demonstrated that JMJD6 and Brd4 interact with distinct

(H and I) Brd4 is required for JMJD6 binding on chromatin, but not vice versa. Standard ChIP assay was performed with anti-JMJD6 (H) or anti-Brd4 (I) antibody in HEK293T cells. The five regions bound by both JMJD6 and Brd4 tested were selected from Figure S3B. ChIP signals were presented as percentage of inputs (±SEM, ***$p < 0.001$). (1:chr1:232,701,545–232,701,745; 2:chr4:12,251,121–12,251,321; 3: chr18:2,832,201–2,832,401; 4: chr3:13,664,851–13,665,051; 5: chr7:61,371,401–61,371,601).
See also Figure S3.

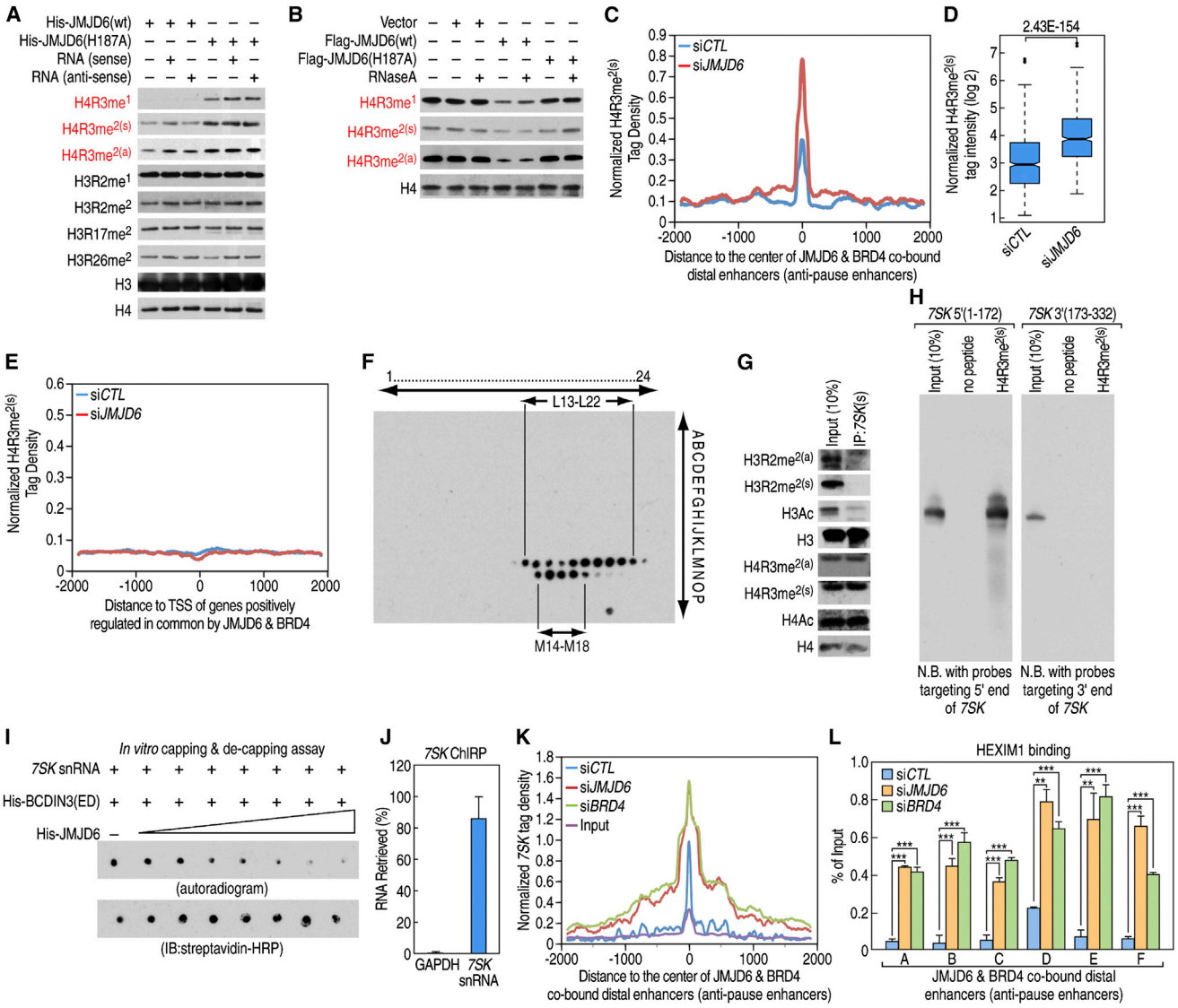

Figure 4. H4R3me and 7SK snRNA Demethylase Activity of JMJD6

(A and B) Histone demethylase activity of JMJD6 examined by in vitro histone demethylase assay using JMJD6 protein purified from bacterial cells (A) or overexpressed HEK293T cells (B).

(C and E) H4R3me$^{2(s)}$ ChIP-seq tag density distribution surrounding the center of JMJD6 and Brd4 cobound distal enhancers (C) or TSS of those JB genes (E).

(D) Box plot showing change of H4R3me$^{2(s)}$ occupancy in (C) is significant (median: 7.73 [siCTL], 14.52 [siJMJD6]).

(F) 7SK snRNA association with modified histone tails detected by Histone Peptide Array. Spot P20 serves as a positive control for IB with HRP-conjugated streptavidin.

(G) 7SK snRNA pull-down mixing in vitro transcribed, biotinylated 7SK snRNA with purified mononucleosomes, followed by IB analysis.

(H) 7SK snRNA association with H4R3me$^{2(s)}$-containing histone tails was examined by in vitro histone peptide pull-down assay. 5′ or 3′ 7SK sequences were incubated with or without H4R3me$^{2(s)}$-containing histone tails. Northern blotting (N.B.) was performed with probes targeting 5′ end (left) or 3′ end (right) of 7SK snRNA.

(I) JMJD6 demethylation of 7SK snRNA examined through in vitro demethylation assay. Equal amount of each reaction was prepared for dot blotting assay followed by autoradiogram or IB with HRP-conjugated streptavidin.

(J) The percentage of cellular 7SK snRNA retrieved by ChIRP. GAPDH served as a negative control. Data were presented as percentage of inputs (±SEM)

(K) 7SK ChIRP tag density distribution surrounding the center of JMJD6 and Brd4 cobound distal enhancers.

(L) Standard ChIP assay was performed with anti-HA antibody in HEK293 cells stably expressing HA-tagged HEXIM1. ChIP signals were presented as percentage of inputs (±SEM, **p < 0.01, ***p < 0.001). JMJD6 and Brd4 cobound distal region A: chr16:30,733,100–30,733,300 (Figure 3F, left); B: chr1:226,632,961–226,633,161 (Figure 3F, right); C: chr1:829,973–830,173 (Figure 5A); D: chr16: 29,940,404–29,940,604 (Figure 5B); E: chr2:19,426,222–19,426,422 (Figure 5C); F: chr22:49,429,007–49,429,207 (Figure S4A).

See also Figure S3.

subunits in the P-TEFb complex, with JMJD6 interacting with CDK9 and Brd4 with Cyclin T1. Furthermore, CDK9 was directly released from the 7SK/HEXIM snRNP by both JMJD6 (1–305) and Brd4 (1209–1362) (regions binding with the P-TEFb complex) (Figure 6C).

To support the hypothesis that both JMJD6 and Brd4 are required to efficiently retain and activate the P-TEFb complex, knockdown of either *JMJD6* or *Brd4* caused a significant decrease of CDK9 occupancy on the promoter regions as well as gene bodies of those JB genes (Figures 6D–6G and S5F–S5G), whereas the CDK9 protein levels remained unchanged (Figure 1F). In accordance with the decrease of CDK9 occupancy, Pol II ser2 phosphorylation decreased significantly across those JB transcription units as well (Figures 6F–6H). We therefore are tempted to suggest a model in which the dual enzymatic activities of JMJD6 act locally to cause dismissal of the 7SK/HEXIM1 inhibitory complex, and the ability of both JMJD6 and Brd4 to retain P-TEFb leads to subsequent Pol II promoter-proximal pause release (Figure 7K).

H4R3me$^{2(s)}$ Demethylation and 7SK Decapping/Demethylation in JMJD6 and Brd4-Mediated Pol II Promoter-Proximal Pause Release

If the dynamic regulation of the identified dual substrates of JMJD6, H4R3me$^{2(s)}$ and 7SK γ-methylphosphate cap, is critical for the release of 7SK/HEXIM1 inhibitory complex imposed on the P-TEFb complex, we would expect to see that knockdown of their corresponding methyltransferases, *PRMT5* and *BCDIN3/MEPCE*, would result in enhanced Pol II promoter-proximal pause release for those JB genes. However, the effect would be expected to be modest due to the fact that these genes are already mostly transcriptionally active. Similar results would also be expected from knocking down the inhibitory components, 7SK snRNA and HEXIM1/2. Knockdown of *PRMT5* in HEK293T cells caused a further decrease of H4R3me$^{2(s)}$ levels on A-PEs (Figures 7A, S6A, and S6B). To support our hypothesis, we observed a significant, although modest, decrease of Pol II TR after *PRMT5* knockdown for JB genes (Figures 7B and 7J). Gro-seq-based TR measurement also supported the inhibitory function of PRMT5 in Pol II promoter-proximal pause release (Figures 7C and 7D). To further strengthen the idea that JMJD6 and PRMT5 antagonize each other in transcriptional pause release control, double knockdown of these two proteins neutralized the TR changes caused by knocking down of each protein individually (Figures 7B and 7J). Together, these data reveal that a dynamic regulation of H4R3me$^{2(s)}$ specifically occurring at A-PEs, with JMJD6 demethylase activity being dominant, is critical for Pol II promoter-proximal pause control.

We next examined the role of decapping/demethylation of 7SK snRNA on Pol II promoter-proximal pause release by knocking down *BCDIN3* followed by Pol II ChIP-seq analysis (Figures 7E and S6C). As expected, knockdown of *BCDIN3* resulted in a significant decrease of 7SK snRNA level (Figure S6D). In support of a role of decapping/demethylation of 7SK snRNA on Pol II promoter-proximal pause release, similar to what was observed for PRMT5, *BCDIN3* knockdown led to a significant, although modest, decrease of Pol II TR for those JB genes (Figures 7F and 7J), which was confirmed by Gro-seq analysis (Figures 7G and 7H). Double knockdown of *JMJD6* and *BCDIN3* neutralized the TR changes caused by knocking down of each protein individually, indicating their antagonistic functions (Figures 7F and 7J). In contrast, double knockdown of *PRMT5* and *BCDIN3* caused an additive effect on TR change, suggesting these two proteins function in parallel to regulate pause release for those JB genes (Figures 7I and 7J). Finally, based on Pol II ChIP-seq and Gro-seq analyses, both *7SK snRNA* and *HEXIM1/2* knockdown caused a significant, although modest, decrease of TR, similar to what observed for other inhibitory components, such as PRMT5 and BCDIN3 (Figures S6E–S6R).

Anti-Pause Enhancers in Other Cell Types

To investigate potential JMJD6 and Brd4 co-occupied anti-pause enhancers in a second cell line, HeLa cells, Gro-seq experiments were performed, and it was found that JMJD6 and Brd4 coregulated a substantial number of genes (n = 844). Significantly, 96% of these genes required both proteins for activation (n = 814), which we referred as JB genes, representing ~83% of the total genes positively regulated by JMJD6 (Figures S7A–S7D). JMJD6 and Brd4 control of Pol II promoter-proximal pause release was readily seen in HeLa cells for those JB genes (Figures S7E and S7F). As was the case in HEK293T cells, Brd4 occupied both promoters and distal regions, whereas JMJD6 bound predominately to distal regions in HeLa cells (Figures S7G and S7H). Importantly, JMJD6 and Brd4 were highly correlated on distal regions (Figures S7I and S7J). Only ~13% of those JB genes had detectable JMJD6 peaks on their promoter regions, suggesting that JMJD6 regulates Pol II promoter-proximal pause release based on the actions at distal sites (Figures S7K and S7L).

To characterize JMJD6 and Brd4 cobound distal sites (anti-pause enhancers), we performed ChIP-seq for H3Ac and H4Ac and examined several data sets from the Encode project in HeLa cells. It was found that, similar to our findings in HEK293T cells, JMJD6 and Brd4 cobound distal sites represented active enhancers (enriched with H3K4me$^{1/2}$ and H3K27Ac, but exhibiting relatively low levels of H3K4me^{3}) with both H3Ac and H4Ac histone marks (Figure S7L). These data suggest that anti-pause enhancer-associated JMJD6 and Brd4 regulation of Pol II promoter-proximal pause release occurs in many cell types.

DISCUSSION

Brd4 and JMJD6 Regulate Promoter-Proximal Pause Release

The evidence presented in this manuscript suggests that JMJD6 and Brd4, acting as functional partners, regulate Pol II promoter-proximal pausing in a large subset of genes based on their actions on distal enhancers, termed *anti-p*ause *e*nhancers (A-PEs). Mechanistically, it appears that acetylated histone H4/H3-mediated, Brd4-dependent binding of JMJD6, an enzyme that displays dual demethylase activities toward both histone arginine and the 7SK snRNA cap, on these A-PEs leads to the release of 7SK snRNA/HEXIM1 inhibitory complex imposed on P-TEFb. Meanwhile, both JMJD6 and Brd4 are capable of

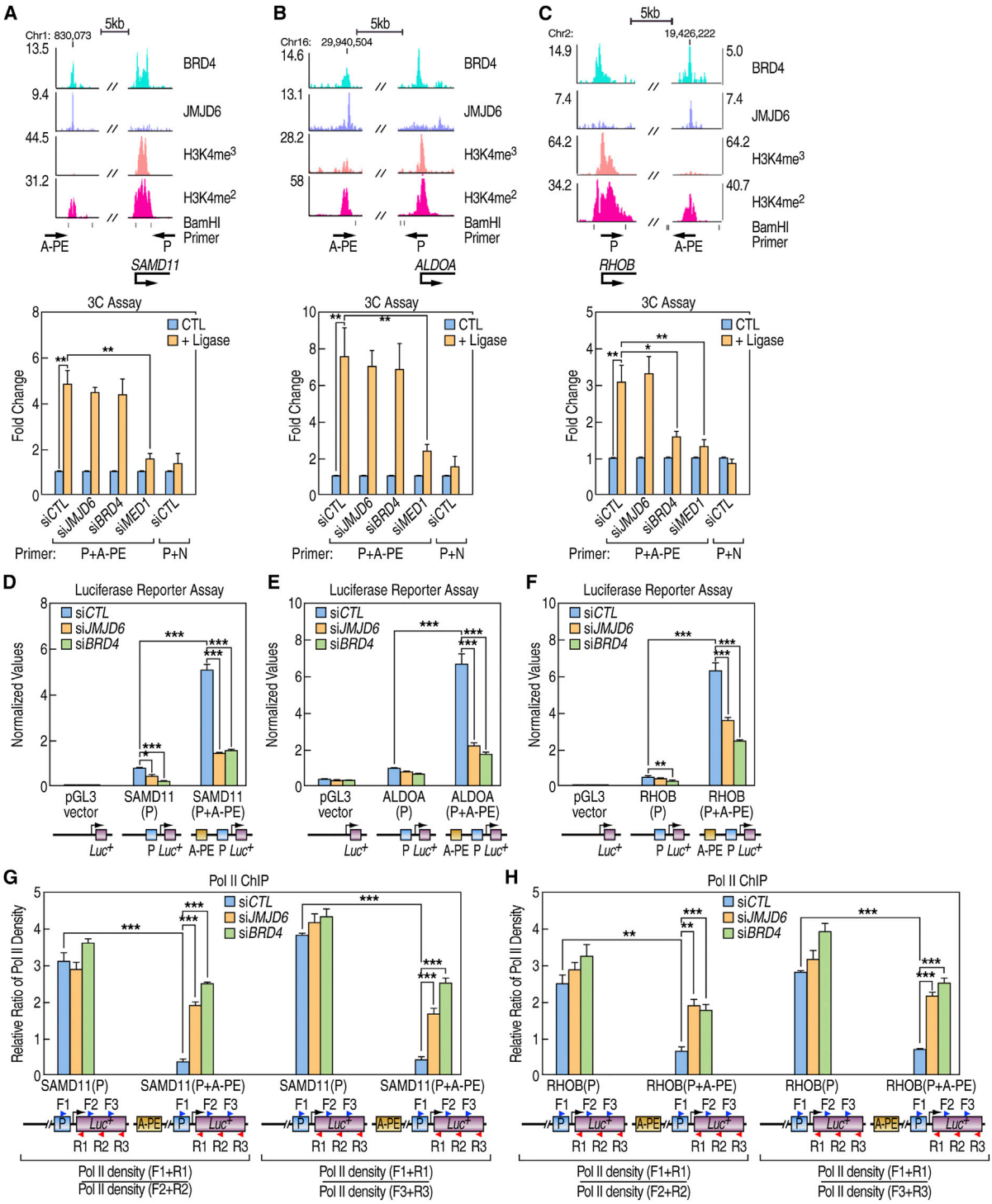

Figure 5. Anti-Pause Enhancers Are Functionally Connected to Coding Gene Promoters

(A–C) Interactions between selected promoter regions (P), *SAMD11* (A), *ALDOA* (B), or *RHOB* (C) and anti-pause enhancers (A-PEs) detected by 3C analysis. Interaction intensity was measured by qPCR using validated primers specific for the tested regions following 3C samples preparation. Data were presented as fold enrichment over 3C samples without adding T4 ligase after normalization to input (±SEM, *p < 0.05, **p < 0.01, ***p < 0.001). A genomic region around 20 kb from each A-PE served as a negative control (N). Center of enhancer: chr1:830,073 (A); chr16:29,940,504 (B); chr2:19,426,322 (C).

(D–F) Luciferase reporter activities driven by selected promoter sequences and A-PEs. HEK293T cells were transfected with control luciferase vector, luciferase vector containing promoter sequence only (P), or both promoter sequence and its corresponding nearby A-PE (P+A), followed by luciferase activity measurement. Data were normalized to Renilla internal control (±SEM, *p < 0.05, **p < 0.01, ***p < 0.001).

(legend continued on next page)

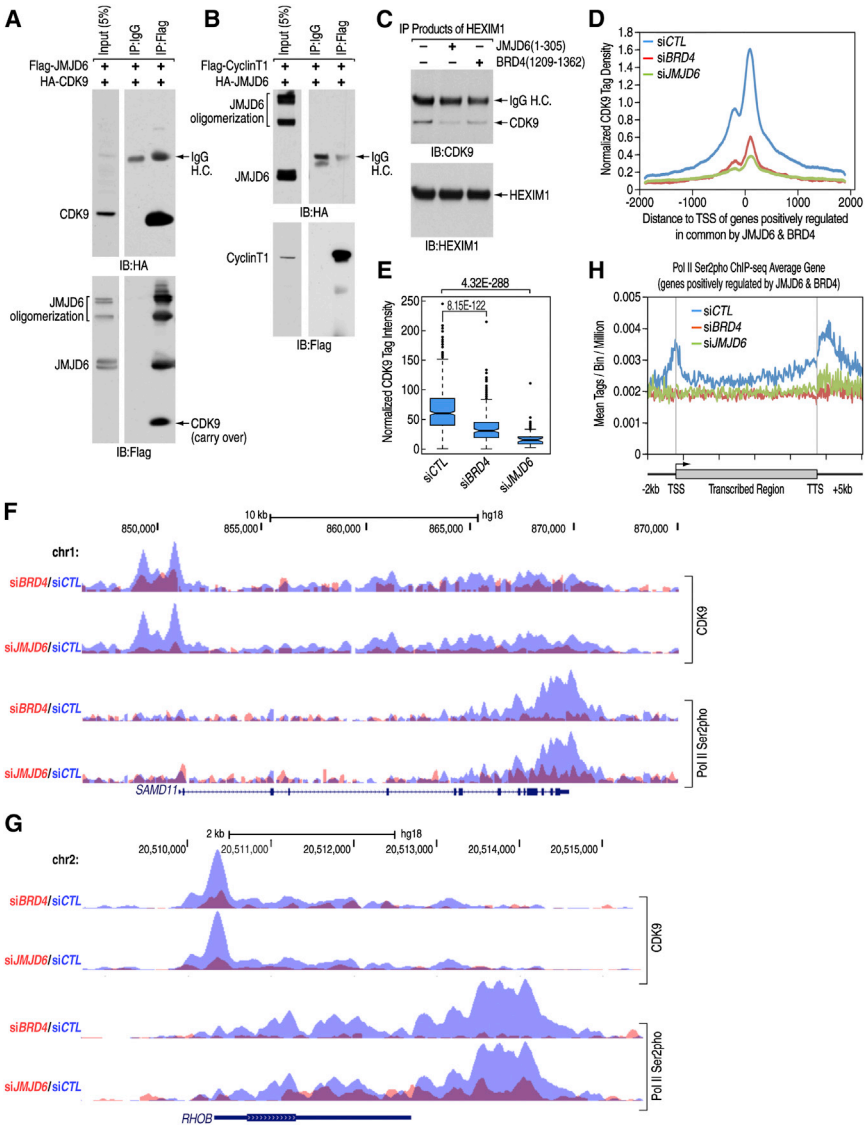

Figure 6. Activation of the P-TEFb Complex by JMJD6 and Brd4

(A and B) JMJD6 interaction with CDK9 (A) or Cyclin T1 (B) examined by IP in HEK293T cells. IgG, immunoglobulin G; H.C., IgG heavy chain.

(C) Release of the P-TEFb complex by JMJD6 or Brd4 protein examined by in vitro P-TEFb release assay.

(D) CDK9 ChIP-seq tag distribution surrounding TSS of those JB genes in HEK293T cells.

(E) Box plot showing change of CDK9 occupancy in (D) is significant (median: 61.39 [siCTL], 32.90 [siBrd4], 15.62 [siJMJD6]).

(F and G) The changes of CDK9 (top) or Pol II ser2 phosphorylation (bottom) occupancy after knocking down of *JMJD6* or *Brd4* were shown for specific genes, as indicated.

(H) Metagenes showing average Pol II ser2 phosphorylation ChIP-seq signals across those JB transcription units. Units are mean tags per bin for 160 bins across the transcribed region of each gene with 2 kb upstream (40 bins of 50 bp each) and 5 kb downstream flanking regions (100 bins of 50 bp each).

See also Figure S5.

extracting and retaining the P-TEFb complex on chromatin, leading to its activation, promoter-proximal Pol II pause release, and gene activation.

Brd4 is required for transcriptional activation of a large number of genes, with many of them also requiring JMJD6 for gene activation. However, a large number of genes exhibiting promoter-proximal pause regulation by Brd4 are independent of JMJD6 for activation. Indeed, the Brd4 interactome contains other functional partners, such as NSD3, that, whereas not required for the Pol II promoter-proximal pause release of those genes jointly regulated by JMJD6 and Brd4 (data not shown), may function for a distinct cohort of genes, based on binding on either promoter regions or distal enhancers (Rahman et al., 2011). Similarly, JMJD6 can function independent on Brd4 in promoter-proximal pause release for other transcription units.

JMJD6: Multiple Substrates, Multiple Functions

In the current study, we have focused on the function of JMJD6 demethylase activity on H4R3me$^{2(s)}$, a repressive histone mark, in promoting transcriptional pause release. As JMJD6 also exhibited demethylase activity toward H4R3me$^{2(a)}$, a histone mark associated with transcriptional activation (Li et al., 2010; Wysocka et al., 2006; Yang et al., 2010), we envision a role of JMJD6 in gene repression. Indeed, our Gro-seq analysis revealed that a subset of genes was repressed by JMJD6. Whether JMJD6 represses gene transcription based on its H4R3me$^{2(a)}$ demethylase activity remains as an interesting question for future investigation. Here, we have also uncovered a JMJD6 enzymatic activity targeting RNA methylation, which is specific to the methyl group in the 7SK snRNA cap structure. Testing

(G and H) Relative ratio of Pol II density in the promoter-proximal region and selected region in the body of luciferase gene. HEK293T cells were transfected with control siRNA or siRNA specifically targeting *JMJD6* or *Brd4* in the presence of luciferase report vector containing promoter sequence only (P) or both promoter sequence and A-PE (P+A) followed by Pol II ChIP analysis. qPCR was performed with primers as indicated, with primer set F1+R1 targeting promoter region, whereas F2+R2 and F3+R3 targeting two distinct regions on luciferase gene body. Data were presented as relative ratio of Pol II density (±SEM, $^{**}p < 0.01$, $^{***}p < 0.001$).

See also Figure S4.

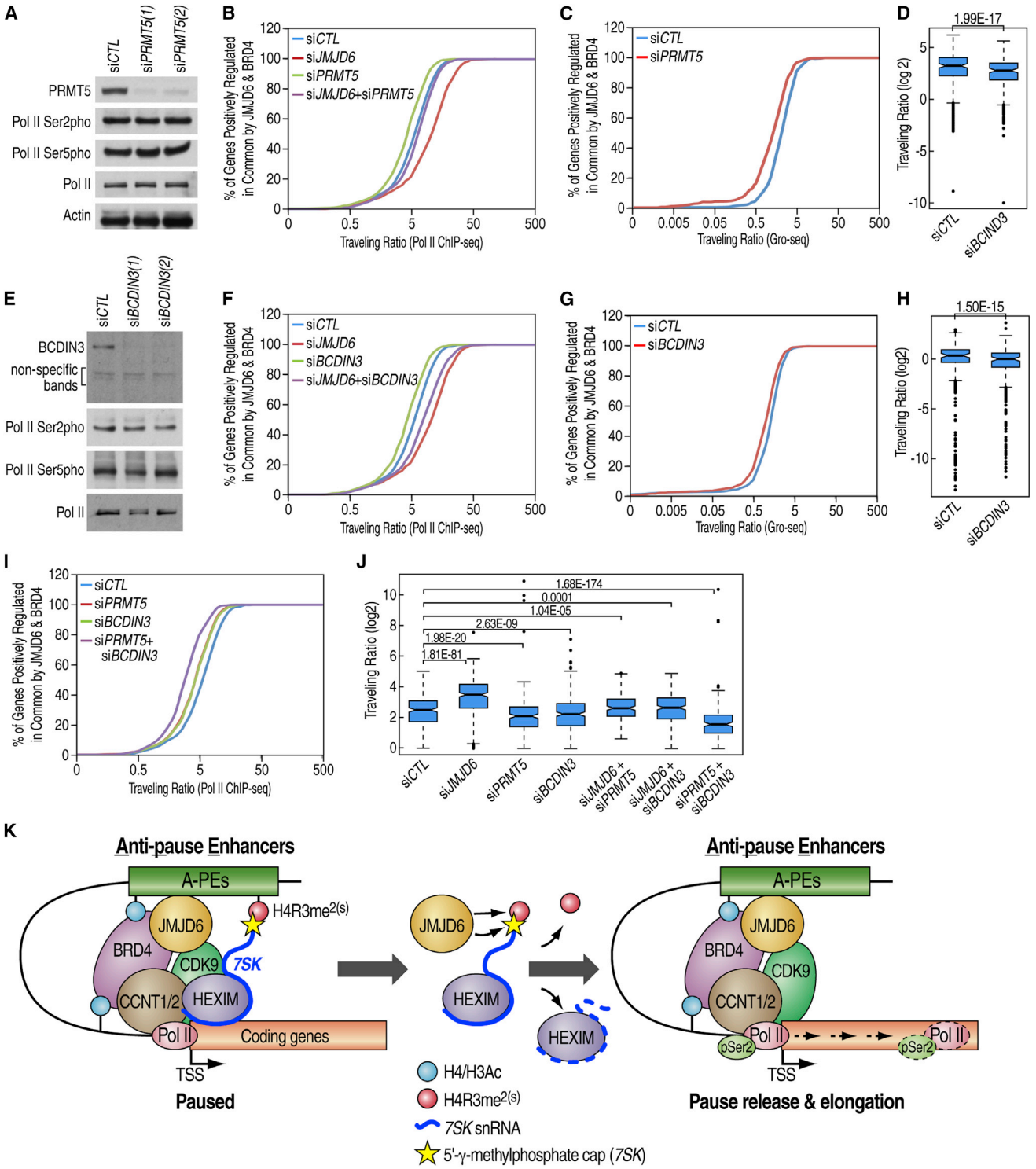

Figure 7. H4R3me$^{2(s)}$ Methylation and 7SK RNA Methylation in Its Cap Structure Are Involved in JMJD6 and Brd4-Mediated Pol II Promoter-Proximal Pause Release

(A and E) HEK293T cells transfected with control siRNA or two independent siRNAs specifically targeting *PRMT5* (A) or *BCDIN3* (E) were subjected to IB analyses.

(B, F, and I) Pol II TR distribution for JB genes in HEK293T cells transfected with siRNA(s) as indicated. Note that experiments shown in (B), (F), and (I) and Figure S2M were performed at the same time.

(C and G) TR distribution based on Gro-seq analysis for JB genes in HEK293T cells transfected with control siRNA or siRNA specifically targeting *PRMT5* (C) or *BCDIN3* (G).

(legend continued on next page)

whether other JmjC-domain-containing proteins target to other types of methylation found on single-stranded RNA (ssRNA) including m^3U and N^6A methylation will be of particular interest for future studies. It is noteworthy that JMJD6 demethylase activities toward both H4R3me$^{2(a)}$ and methyl group in the 7SK snRNA cap structure occur locally on chromatin, suggesting that other demethylases with similar activities might exist, which is also consistent with the fact that, despite being born with severe developmental defects, viable *JMJD6* knockout mice could be identified at birth (Böse et al., 2004; Kunisaki et al., 2004; Li et al., 2003).

7SK snRNA: A Noncoding RNA Reading Histone Marks

Our data support the idea that 7SK snRNA/HEXIM/P-TEFb is tethered to chromatin through 7SK snRNA recognition of the H4R3me$^{2(s)}$ mark on A-PEs. JMJD6/Brd4 protein complex erasure of H4R3me$^{2(s)}$ releases 7SK snRNA/HEXIM inhibition, allowing local P-TEFb activation to occur. Reading of other histone marks on chromatin, by 7SK snRNA, may also contribute to its function in transcriptional regulation. Indeed, a specific locked nucleic acid (LNA) targeting 7SK dramatically affects Pol II promoter-proximal pause release and transcription of a large set of genes.

In conclusion, our studies here have revealed anti-pause enhancers regulate Pol II promoter-proximal pause release, on which: (1) JMJD6 and Brd4 binding is detected; (2) there is enrichment of H4Ac and H3Ac marks, as well as classical active enhancer marks; (3) release of 7SK snRNA/HEXIM inhibitory complex occurs, in response to JMJD6 enzymatic activity targeting both H4R3me$^{2(s)}$ and/or 7SK snRNA cap; and (4) looping is formed with coding gene promoters, providing the apparent architectural basis for their ability to regulate transcriptional pause release events at promoters. A-PEs, therefore, apparently are enhancers with a function in transcriptional pause release, with their unique feature being cobound by both JMJD6 and Brd4, and the associated molecular mechanisms.

EXPERIMENTAL PROCEDURES

siRNA Transfection, RNA Isolation, and qRT-PCR

Two independent siRNAs against *JMJD6*, *Brd4*, *PRMT5*, *BCDIN3*, *HEXIM1*, or *HEXIM2* were used in this study (see Extended Experimental Procedures for siRNA sequence information). Locked nucleic acid (LNA) targeting 7SK snRNA was designed and purchased form Exiqon (G*A*G*A*G*C*T*T*G*T*T*T*G*G*A*G [* = phosphorothioate]). siRNA and LNA transfections were performed using Lipofectamine 2000 (Invitrogen) according to the manufacturer's protocol. Transfection efficiency was determined by immunoblotting and/or qRT-PCR. Total RNA was isolated from HEK293T cells using RNeasy Mini Kit (QIAGEN) following the manufacturer's protocol. First-strand cDNA synthesis from total RNA was carried out using SuperScript III First-strand cDNA synthesis system (Invitrogen). Resulting cDNA was then analyzed by quantitative PCR (qPCR) using Stratagene Mx3000 machine. Primers are specific for genes tested and their sequences are available upon request. All qRT-PCRs were repeated at least three times, and representative results are shown.

Traveling Ratio Calculation

Pol II TR was defined as the relative ratio of Pol II density in the promoter-proximal region and the gene body. The promoter proximal region refers to the window from −50 to +300 bp surrounding transcription start site (TSS). Gene body is from 300 bp downstream of TSS to the annotated end. TR calculated based on Gro-seq tag density was defined as ratio of Gro-seq reads density at the promoter-proximal bin (from −50 to +300 bp surrounding TSS) to Gro-seq density at the gene body bin (from +300 bp to the annotated end). The significance of the change of TR between control and knockdown samples was displayed using box plot and determined using Student's t test.

ACCESSION NUMBERS

The GEO accession number for ChIP-seq and Gro-seq data sets reported in this paper is GSE51633.

SUPPLEMENTAL INFORMATION

Supplemental Information includes Extended Experimental Procedures, seven figures, and four tables and can be found with this article online at http://dx.doi.org/10.1016/j.cell.2013.10.056.

ACKNOWLEDGMENTS

We thank Dr. Thomas M. Vondriska at UCLA for mass spectrometry analysis to identify JMJD6-associated proteins. We thank Janet Hightower for assistance with figure preparation. M.G.R. is an Investigator with the Howard Hughes Medical Institute. This work was supported by NIH grants (NS34934, DK39949, DK18477, CA173903, HL065445, and DK097748) to M.G.R. W.L. is the recipient of a Susan Komen for the Cure Postdoctoral Fellowship (PDF12229881).

Received: March 5, 2013
Revised: September 3, 2013
Accepted: October 23, 2013
Published: December 19, 2013

REFERENCES

Adelman, K., and Lis, J.T. (2012). Promoter-proximal pausing of RNA polymerase II: emerging roles in metazoans. Nat. Rev. Genet. *13*, 720–731.

Anand, P., Brown, J.D., Lin, C.Y., Qi, J., Zhang, R., Artero, P.C., Alaiti, M.A., Bullard, J., Alazem, K., Margulies, K.B., et al. (2013). BET bromodomains mediate transcriptional pause release in heart failure. Cell *154*, 569–582.

Böse, J., Gruber, A.D., Helming, L., Schiebe, S., Wegener, I., Hafner, M., Beales, M., Köntgen, F., and Lengeling, A. (2004). The phosphatidylserine

(D and H) Box plots showing that the change of Pol II TR caused by knockdown of *PRMT5* or *BCDIN3* as shown in (C) or (G), respectively. Median (E): 2.10 (siCTL), 1.30 (siPRMT5); median (J): 1.33 (siCTL), 1.01 (siPRMT5).

(J) Box plot showing change of Pol II TR as shown in (B), (F), and (I). Median: 5.65 (siCTL), 11.38 (siJMJD6), 4.30 (siPRMT5), 4.41 (siBCDIN3), 6.24 (siJMJD6+siPRMT5), 6.35 (siJMJD6+siBCDIN3), 2.86 (siPRMT5+siBCDIN3).

(K) (Model) regulation of transcriptional pause release of a subset of transcriptional units by JMJD6-associated dual enzymatic activities on distal A-PEs. 7SK snRNA/HEXIM-associated inactive P-TEFb complex was tethered to chromatin through 7SK snRNA reading of H4R3me$^{2(s)}$ mark. H4Ac and/or H3Ac-mediated recruitment of JMJD6/Brd4 protein complex exhibits dual enzymatic activities, both histone demethylation activity targeting H4R3me$^{2(s)}$ and RNA demethylation activity targeting 7SK snRNA methyl group in its cap structure, resulting in the dismissal of the 7SK snRNA/HEXIM inhibitory complex imposed on P-TEFb. Meanwhile, the ability of both JMJD6 and Brd4 to interact with P-TEFb complex retains its association with chromatin and permits subsequent pause release for transcriptional elongation.

See also Figures S6 and S7.

receptor has essential functions during embryogenesis but not in apoptotic cell removal. J. Biol. *3*, 15.

Chang, B., Chen, Y., Zhao, Y., and Bruick, R.K. (2007). JMJD6 is a histone arginine demethylase. Science *318*, 444–447.

Cui, P., Qin, B., Liu, N., Pan, G., and Pei, D. (2004). Nuclear localization of the phosphatidylserine receptor protein via multiple nuclear localization signals. Exp. Cell Res. *293*, 154–163.

Delmore, J.E., Issa, G.C., Lemieux, M.E., Rahl, P.B., Shi, J., Jacobs, H.M., Kastritis, E., Gilpatrick, T., Paranal, R.M., Qi, J., et al. (2011). BET bromodomain inhibition as a therapeutic strategy to target c-Myc. Cell *146*, 904–917.

Dey, A., Nishiyama, A., Karpova, T., McNally, J., and Ozato, K. (2009). Brd4 marks select genes on mitotic chromatin and directs postmitotic transcription. Mol. Biol. Cell *20*, 4899–4909.

Fadok, V.A., Bratton, D.L., Rose, D.M., Pearson, A., Ezekewitz, R.A., and Henson, P.M. (2000). A receptor for phosphatidylserine-specific clearance of apoptotic cells. Nature *405*, 85–90.

Filippakopoulos, P., Qi, J., Picaud, S., Shen, Y., Smith, W.B., Fedorov, O., Morse, E.M., Keates, T., Hickman, T.T., Felletar, I., et al. (2010). Selective inhibition of BET bromodomains. Nature *468*, 1067–1073.

Gyuris, A., Donovan, D.J., Seymour, K.A., Lovasco, L.A., Smilowitz, N.R., Halperin, A.L., Klysik, J.E., and Freiman, R.N. (2009). The chromatin-targeting protein Brd2 is required for neural tube closure and embryogenesis. Biochim. Biophys. Acta *1789*, 413–421.

Hah, N., Murakami, S., Nagari, A., Danko, C.G., and Kraus, W.L. (2013). Enhancer transcripts mark active estrogen receptor binding sites. Genome Res. *23*, 1210–1223.

Hargreaves, D.C., Horng, T., and Medzhitov, R. (2009). Control of inducible gene expression by signal-dependent transcriptional elongation. Cell *138*, 129–145.

Heintzman, N.D., Hon, G.C., Hawkins, R.D., Kheradpour, P., Stark, A., Harp, L.F., Ye, Z., Lee, L.K., Stuart, R.K., Ching, C.W., et al. (2009). Histone modifications at human enhancers reflect global cell-type-specific gene expression. Nature *459*, 108–112.

Hong, X., Zang, J., White, J., Wang, C., Pan, C.H., Zhao, R., Murphy, R.C., Dai, S., Henson, P., Kappler, J.W., et al. (2010). Interaction of JMJD6 with single-stranded RNA. Proc. Natl. Acad. Sci. USA *107*, 14568–14572.

Houzelstein, D., Bullock, S.L., Lynch, D.E., Grigorieva, E.F., Wilson, V.A., and Beddington, R.S. (2002). Growth and early postimplantation defects in mice deficient for the bromodomain-containing protein Brd4. Mol. Cell. Biol. *22*, 3794–3802.

Jang, M.K., Mochizuki, K., Zhou, M., Jeong, H.S., Brady, J.N., and Ozato, K. (2005). The bromodomain protein Brd4 is a positive regulatory component of P-TEFb and stimulates RNA polymerase II-dependent transcription. Mol. Cell *19*, 523–534.

Jeronimo, C., Forget, D., Bouchard, A., Li, Q., Chua, G., Poitras, C., Thérien, C., Bergeron, D., Bourassa, S., Greenblatt, J., et al. (2007). Systematic analysis of the protein interaction network for the human transcription machinery reveals the identity of the 7SK capping enzyme. Mol. Cell *27*, 262–274.

Kagey, M.H., Newman, J.J., Bilodeau, S., Zhan, Y., Orlando, D.A., van Berkum, N.L., Ebmeier, C.C., Goossens, J., Rahl, P.B., Levine, S.S., et al. (2010). Mediator and cohesin connect gene expression and chromatin architecture. Nature *467*, 430–435.

Kim, J.B., and Sharp, P.A. (2001). Positive transcription elongation factor B phosphorylates hSPT5 and RNA polymerase II carboxyl-terminal domain independently of cyclin-dependent kinase-activating kinase. J. Biol. Chem. *276*, 12317–12323.

Krueger, B.J., Varzavand, K., Cooper, J.J., and Price, D.H. (2010). The mechanism of release of P-TEFb and HEXIM1 from the 7SK snRNP by viral and cellular activators includes a conformational change in 7SK. PLoS ONE *5*, e12335.

Kunisaki, Y., Masuko, S., Noda, M., Inayoshi, A., Sanui, T., Harada, M., Sasazuki, T., and Fukui, Y. (2004). Defective fetal liver erythropoiesis and T lymphopoiesis in mice lacking the phosphatidylserine receptor. Blood *103*, 3362–3364.

Lachner, M., O'Sullivan, R.J., and Jenuwein, T. (2003). An epigenetic road map for histone lysine methylation. J. Cell Sci. *116*, 2117–2124.

Lam, M.T., Cho, H., Lesch, H.P., Gosselin, D., Heinz, S., Tanaka-Oishi, Y., Benner, C., Kaikkonen, M.U., Kim, A.S., Kosaka, M., et al. (2013). Rev-Erbs repress macrophage gene expression by inhibiting enhancer-directed transcription. Nature *498*, 511–515.

Li, M.O., Sarkisian, M.R., Mehal, W.Z., Rakic, P., and Flavell, R.A. (2003). Phosphatidylserine receptor is required for clearance of apoptotic cells. Science *302*, 1560–1563.

Li, X., Hu, X., Patel, B., Zhou, Z., Liang, S., Ybarra, R., Qiu, Y., Felsenfeld, G., Bungert, J., and Huang, S. (2010). H4R3 methylation facilitates beta-globin transcription by regulating histone acetyltransferase binding and H3 acetylation. Blood *115*, 2028–2037.

Li, W., Notani, D., Ma, Q., Tanasa, B., Nunez, E., Chen, A.Y., Merkurjev, D., Zhang, J., Ohgi, K., Song, X., et al. (2013). Functional roles of enhancer RNAs for oestrogen-dependent transcriptional activation. Nature *498*, 516–520.

Lovén, J., Hoke, H.A., Lin, C.Y., Lau, A., Orlando, D.A., Vakoc, C.R., Bradner, J.E., Lee, T.I., and Young, R.A. (2013). Selective inhibition of tumor oncogenes by disruption of super-enhancers. Cell *153*, 320–334.

Marshall, N.F., Peng, J., Xie, Z., and Price, D.H. (1996). Control of RNA polymerase II elongation potential by a novel carboxyl-terminal domain kinase. J. Biol. Chem. *271*, 27176–27183.

Min, I.M., Waterfall, J.J., Core, L.J., Munroe, R.J., Schimenti, J., and Lis, J.T. (2011). Regulating RNA polymerase pausing and transcription elongation in embryonic stem cells. Genes Dev. *25*, 742–754.

Mochizuki, K., Nishiyama, A., Jang, M.K., Dey, A., Ghosh, A., Tamura, T., Natsume, H., Yao, H., and Ozato, K. (2008). The bromodomain protein Brd4 stimulates G1 gene transcription and promotes progression to S phase. J. Biol. Chem. *283*, 9040–9048.

Natoli, G., and Andrau, J.C. (2012). Noncoding transcription at enhancers: general principles and functional models. Annu. Rev. Genet. *46*, 1–19.

Nguyen, V.T., Kiss, T., Michels, A.A., and Bensaude, O. (2001). 7SK small nuclear RNA binds to and inhibits the activity of CDK9/cyclin T complexes. Nature *414*, 322–325.

Nicodeme, E., Jeffrey, K.L., Schaefer, U., Beinke, S., Dewell, S., Chung, C.W., Chandwani, R., Marazzi, I., Wilson, P., Coste, H., et al. (2010). Suppression of inflammation by a synthetic histone mimic. Nature *468*, 1119–1123.

Rahl, P.B., Lin, C.Y., Seila, A.C., Flynn, R.A., McCuine, S., Burge, C.B., Sharp, P.A., and Young, R.A. (2010). c-Myc regulates transcriptional pause release. Cell *141*, 432–445.

Rahman, S., Sowa, M.E., Ottinger, M., Smith, J.A., Shi, Y., Harper, J.W., and Howley, P.M. (2011). The Brd4 extraterminal domain confers transcription activation independent of pTEFb by recruiting multiple proteins, including NSD3. Mol. Cell. Biol. *31*, 2641–2652.

Ren, B. (2010). Transcription: Enhancers make non-coding RNA. Nature *465*, 173–174.

Reppas, N.B., Wade, J.T., Church, G.M., and Struhl, K. (2006). The transition between transcriptional initiation and elongation in E. coli is highly variable and often rate limiting. Mol. Cell *24*, 747–757.

Ruthenburg, A.J., Li, H., Patel, D.J., and Allis, C.D. (2007). Multivalent engagement of chromatin modifications by linked binding modules. Nat. Rev. Mol. Cell Biol. *8*, 983–994.

Shumyatsky, G.P., Tillib, S.V., and Kramerov, D.A. (1990). B2 RNA and 7SK RNA, RNA polymerase III transcripts, have a cap-like structure at their 5′ end. Nucleic Acids Res. *18*, 6347–6351.

Tibrewal, N., Liu, T., Li, H., and Birge, R.B. (2007). Characterization of the biochemical and biophysical properties of the phosphatidylserine receptor (PS-R) gene product. Mol. Cell. Biochem. *304*, 119–125.

Wada, T., Takagi, T., Yamaguchi, Y., Watanabe, D., and Handa, H. (1998). Evidence that P-TEFb alleviates the negative effect of DSIF on RNA polymerase II-dependent transcription in vitro. EMBO J. *17*, 7395–7403.

Webby, C.J., Wolf, A., Gromak, N., Dreger, M., Kramer, H., Kessler, B., Nielsen, M.L., Schmitz, C., Butler, D.S., Yates, J.R., 3rd., et al. (2009). Jmjd6 catalyses lysyl-hydroxylation of U2AF65, a protein associated with RNA splicing. Science *325*, 90–93.

Wu, S.Y., Zhou, T., and Chiang, C.M. (2003). Human mediator enhances activator-facilitated recruitment of RNA polymerase II and promoter recognition by TATA-binding protein (TBP) independently of TBP-associated factors. Mol. Cell. Biol. *23*, 6229–6242.

Wysocka, J., Allis, C.D., and Coonrod, S. (2006). Histone arginine methylation and its dynamic regulation. Front. Biosci. *11*, 344–355.

Xu, X., Hoang, S., Mayo, M.W., and Bekiranov, S. (2010). Application of machine learning methods to histone methylation ChIP-Seq data reveals H4R3me2 globally represses gene expression. BMC Bioinformatics *11*, 396.

Yamada, T., Yamaguchi, Y., Inukai, N., Okamoto, S., Mura, T., and Handa, H. (2006). P-TEFb-mediated phosphorylation of hSpt5 C-terminal repeats is critical for processive transcription elongation. Mol. Cell *21*, 227–237.

Yang, Z., Zhu, Q., Luo, K., and Zhou, Q. (2001). The 7SK small nuclear RNA inhibits the CDK9/cyclin T1 kinase to control transcription. Nature *414*, 317–322.

Yang, Z., Yik, J.H., Chen, R., He, N., Jang, M.K., Ozato, K., and Zhou, Q. (2005). Recruitment of P-TEFb for stimulation of transcriptional elongation by the bromodomain protein Brd4. Mol. Cell *19*, 535–545.

Yang, Z., He, N., and Zhou, Q. (2008). Brd4 recruits P-TEFb to chromosomes at late mitosis to promote G1 gene expression and cell cycle progression. Mol. Cell. Biol. *28*, 967–976.

Yang, Y., Lu, Y., Espejo, A., Wu, J., Xu, W., Liang, S., and Bedford, M.T. (2010). TDRD3 is an effector molecule for arginine-methylated histone marks. Mol. Cell *40*, 1016–1023.

Yang, L., Lin, C., Liu, W., Zhang, J., Ohgi, K.A., Grinstein, J.D., Dorrestein, P.C., and Rosenfeld, M.G. (2011). ncRNA- and Pc2 methylation-dependent gene relocation between nuclear structures mediates gene activation programs. Cell *147*, 773–788.

Zeitlinger, J., Stark, A., Kellis, M., Hong, J.W., Nechaev, S., Adelman, K., Levine, M., and Young, R.A. (2007). RNA polymerase stalling at developmental control genes in the Drosophila melanogaster embryo. Nat. Genet. *39*, 1512–1516.

Zuber, J., Shi, J., Wang, E., Rappaport, A.R., Herrmann, H., Sison, E.A., Magoon, D., Qi, J., Blatt, K., Wunderlich, M., et al. (2011). RNAi screen identifies Brd4 as a therapeutic target in acute myeloid leukaemia. Nature *478*, 524–528.